Supplementary figures

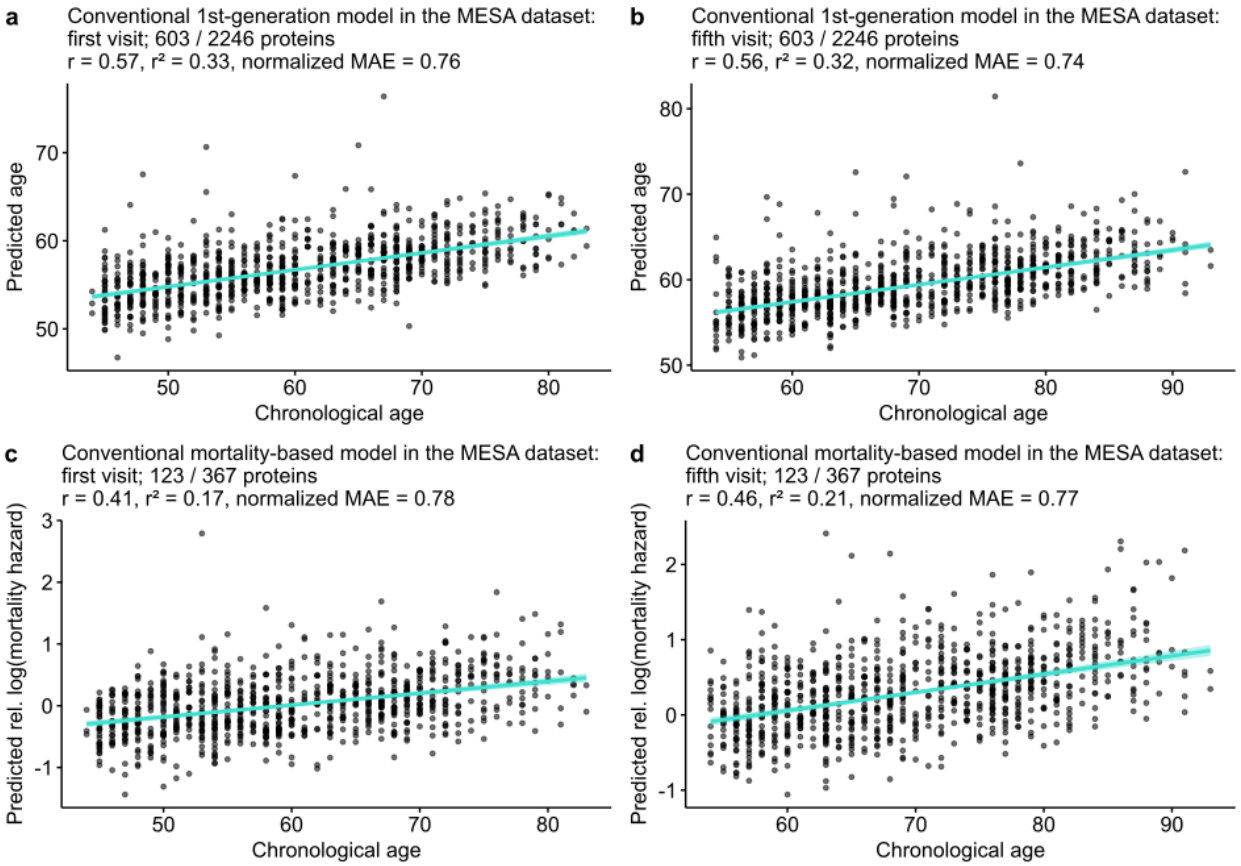

Supplementary Figure 1. The conventional 1st-generation model and the conventional mortality-based model predict chronological age in the SomaScan proteomics from the external MESA study (Bild et al., 2002), even if not all proteins are present in the dataset. a – b. Biological age as predicted by our 1st-generation proteome aging model has a strong positive correlation with chronological age in the MESA dataset, both in the SomaScan proteomics collected at the first (a) and the fifth visits (b) (*n* = 921 participants each). **c – d.** Biological age as predicted by our mortality-based proteome aging model has a strong positive correlation with chronological age in the MESA dataset, both in the SomaScan proteomics collected at the first (a) and the fifth visits (b) (*n* = 921 participants each). In all panels, the number of proteins from the aging models with non-zero coefficients used in the SomaScan dataset is shown as a fraction of the total number of proteins with non-zero coefficients for the aging models. r: correlation coefficient, r²: coefficient of determination, normalized MAE: mean absolute error of the normalized residuals, magenta: women, blue: men. Robust regression lines with 95% confidence bands (shaded area) are added.

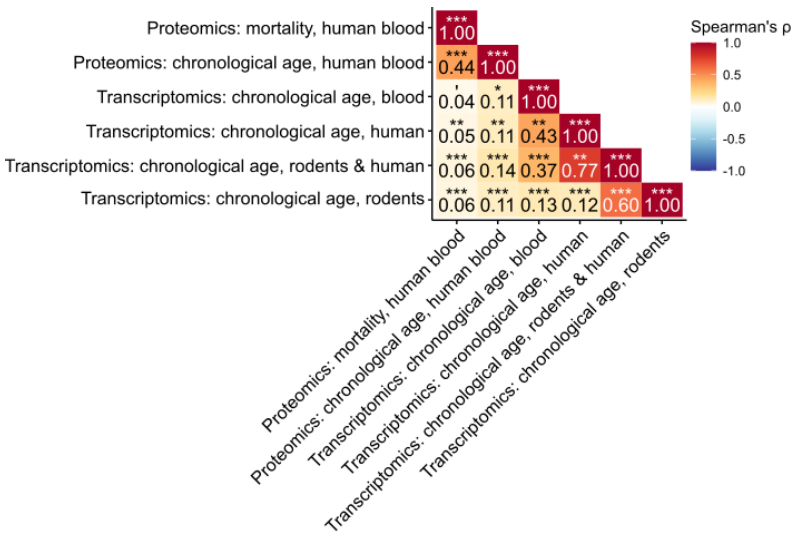

Supplementary Figure 2. Correlation of proteomic and transcriptomic signatures/biomarkers of chronological age and mortality. Heatmap showing the correlation coefficients (r) at the protein- or gene-level between the protein-level analysis for chronological age, the protein-level analysis for mortality, and several transcriptomic associations with chronological age derived from Tyshkovskiy et al. (2023).

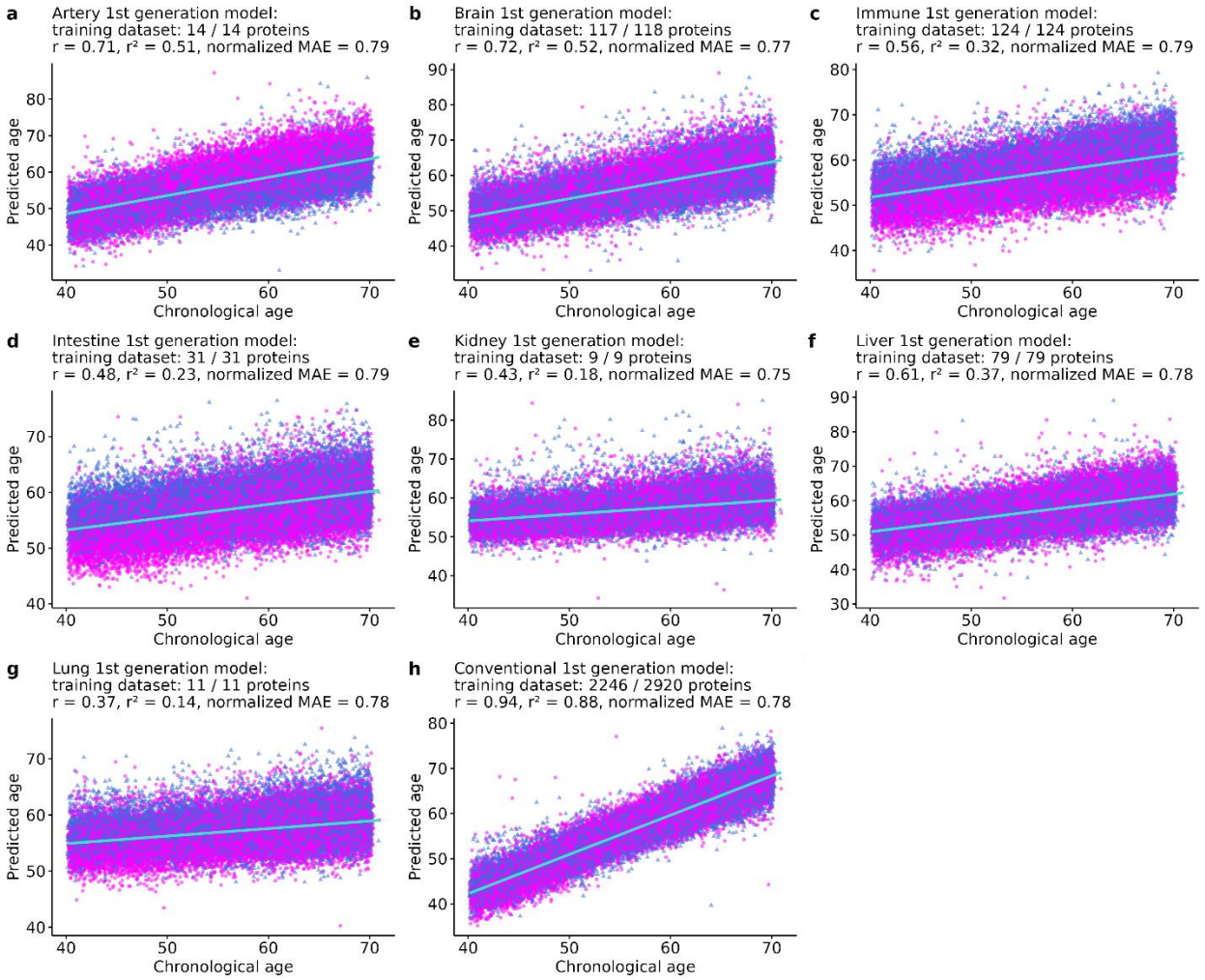

Supplementary Figure 3. Predicted biological age correlates positively with chronological age in the training dataset (*n* = 42,412 UK Biobank participants) for all organ-specific 1st-generation aging models. r: correlation coefficient, r²: coefficient of determination, normalized MAE: mean absolute error of the normalized residuals, magenta: women, blue: men. Robust regression lines with 95% confidence bands (shaded area) are added.

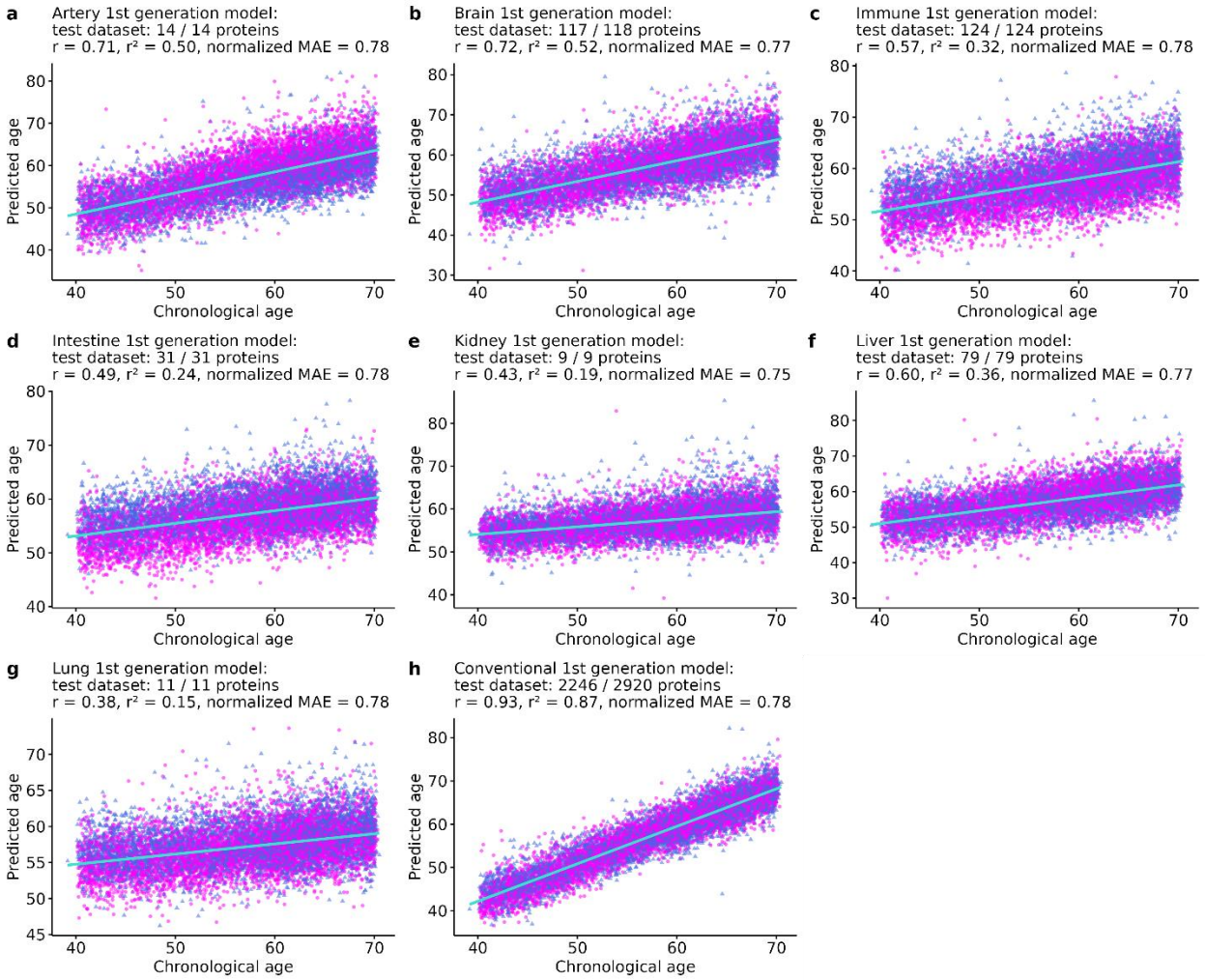

Supplementary Figure 4. Predicted biological age correlates positively with chronological age in the test dataset (*n* = 10,603 UK Biobank participants) for all organ-specific 1st-generation aging models. r: correlation coefficient, r²: coefficient of determination, normalized MAE: mean absolute error of the normalized residuals, magenta: women, blue: men. Robust regression lines with 95% confidence bands (shaded area) are added.

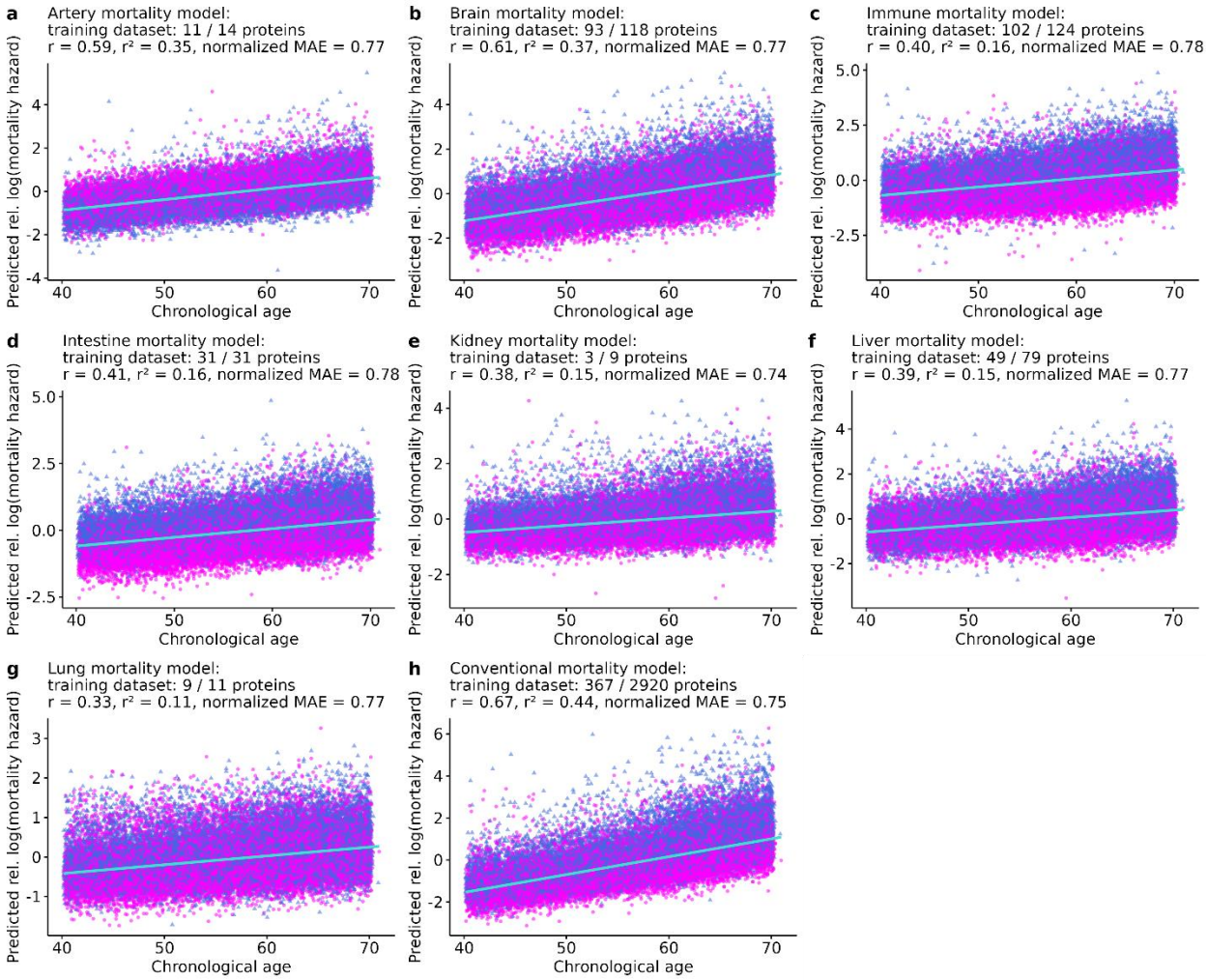

Supplementary Figure 5. Predicted relative log(hazard) of mortality correlates positively with chronological age in the training dataset (*n* = 42,412 UK Biobank participants) for all mortality-based aging models. r: correlation coefficient, r²: coefficient of determination, normalized MAE: mean absolute error of the normalized residuals, magenta: women, blue: men. Robust regression lines with 95% confidence bands (shaded area) are added.

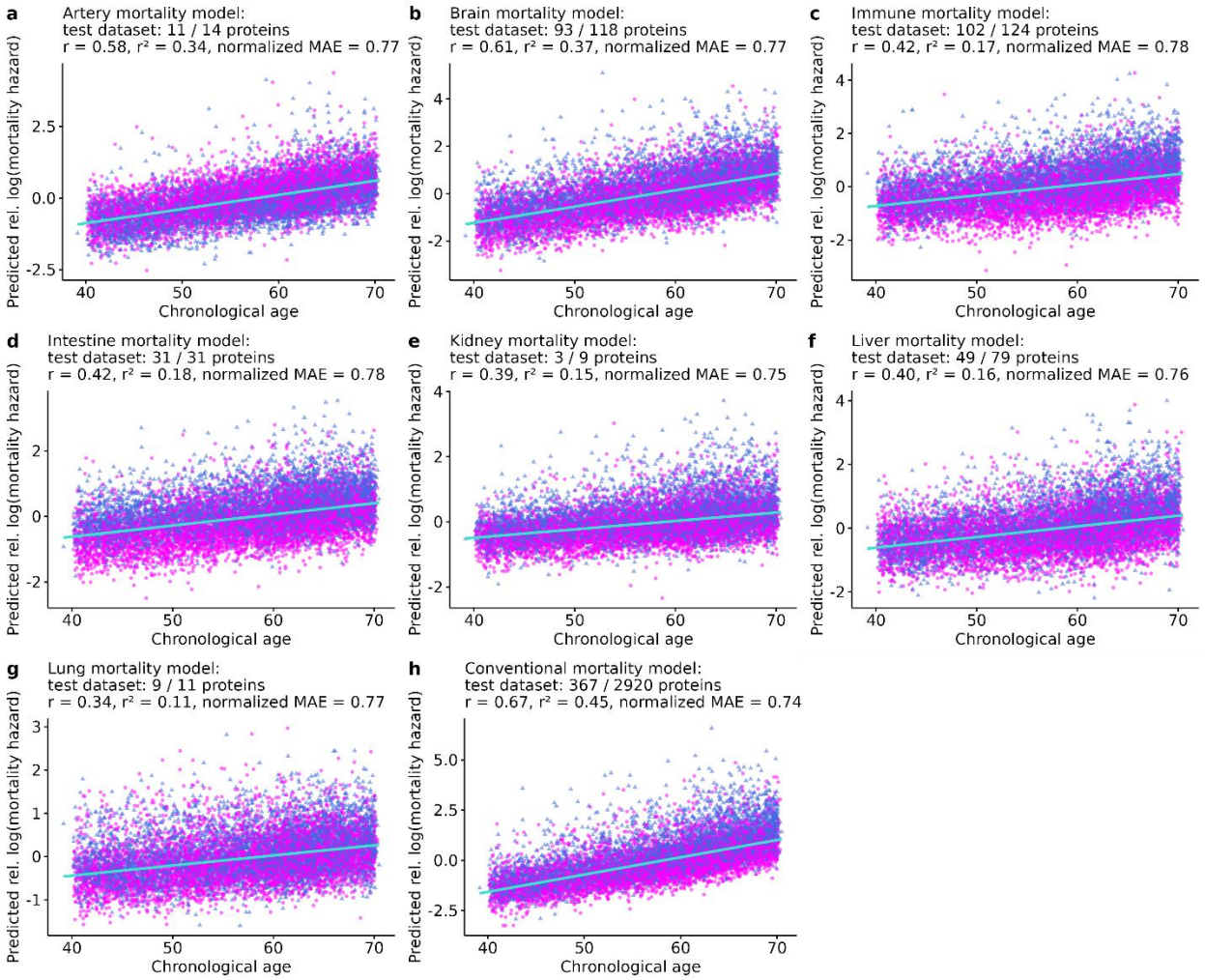

Supplementary Figure 6. Predicted relative log(hazard) of mortality correlates positively with chronological age in the test dataset (*n* = 10,603 UK Biobank participants) for all mortality-based aging models. r: correlation coefficient, r²: coefficient of determination, normalized MAE: mean absolute error of the normalized residuals, magenta: women, blue: men. Robust regression lines with 95% confidence bands (shaded area) are added.

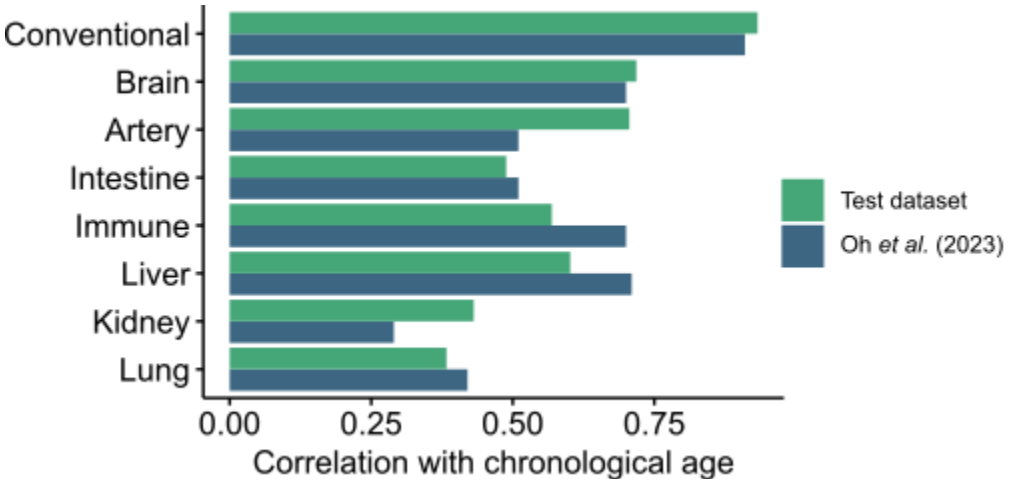

Supplementary Figure 7. Organ-specific aging models predict chronological age. Bar plots showing the correlation coefficients (r) with chronological age for the predicted ages by the conventional and organ-specific 1st-generation aging models in the test dataset (*n* = 10,603 UK Biobank participants), and the correlation coefficients with chronological age reported by Oh et al. (2023).

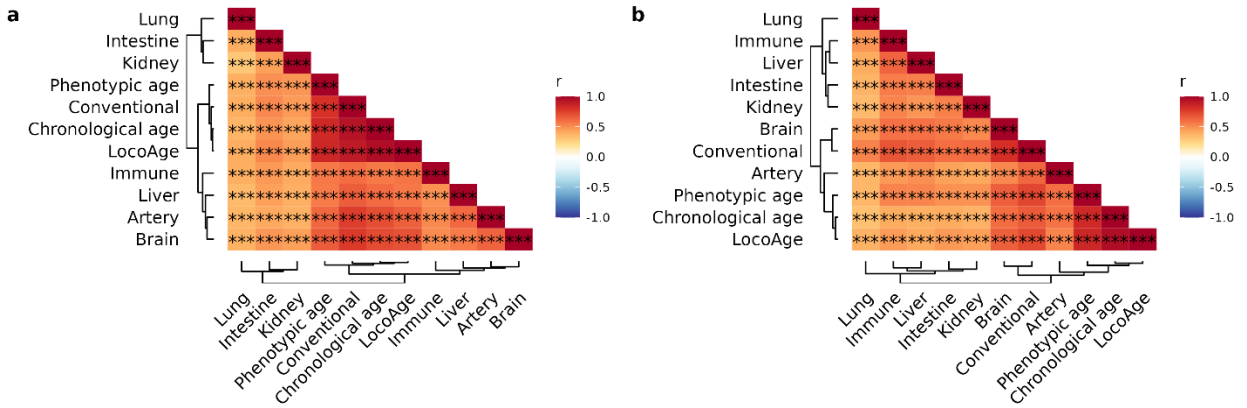

Supplementary Figure 8. Organ-specific aging models correlate with the conventional model, chronological age, phenotypic age and locomotor age. a. Heatmap showing the correlation coefficients (r) for the predicted ages by the organ-specific 1st-generation aging models, the conventional 1st-generation aging model, and chronological age (*n* = 53,015 UK Biobank participants), as well as phenotypic age (*n* = 44,901 UK Biobank participants) and LocoAge (*n* = 10,428 UK Biobank participants). **b.** Heatmap showing the correlation coefficients (r) for the predicted relative log(hazards) of mortality by the mortality-based organ-specific aging models, the conventional mortality-based aging model, and chronological age (*n* = 53,015 UK Biobank participants), as well as phenotypic age (*n* = 44,901 UK Biobank participants) and LocoAge (*n* = 10,428 UK Biobank participants).

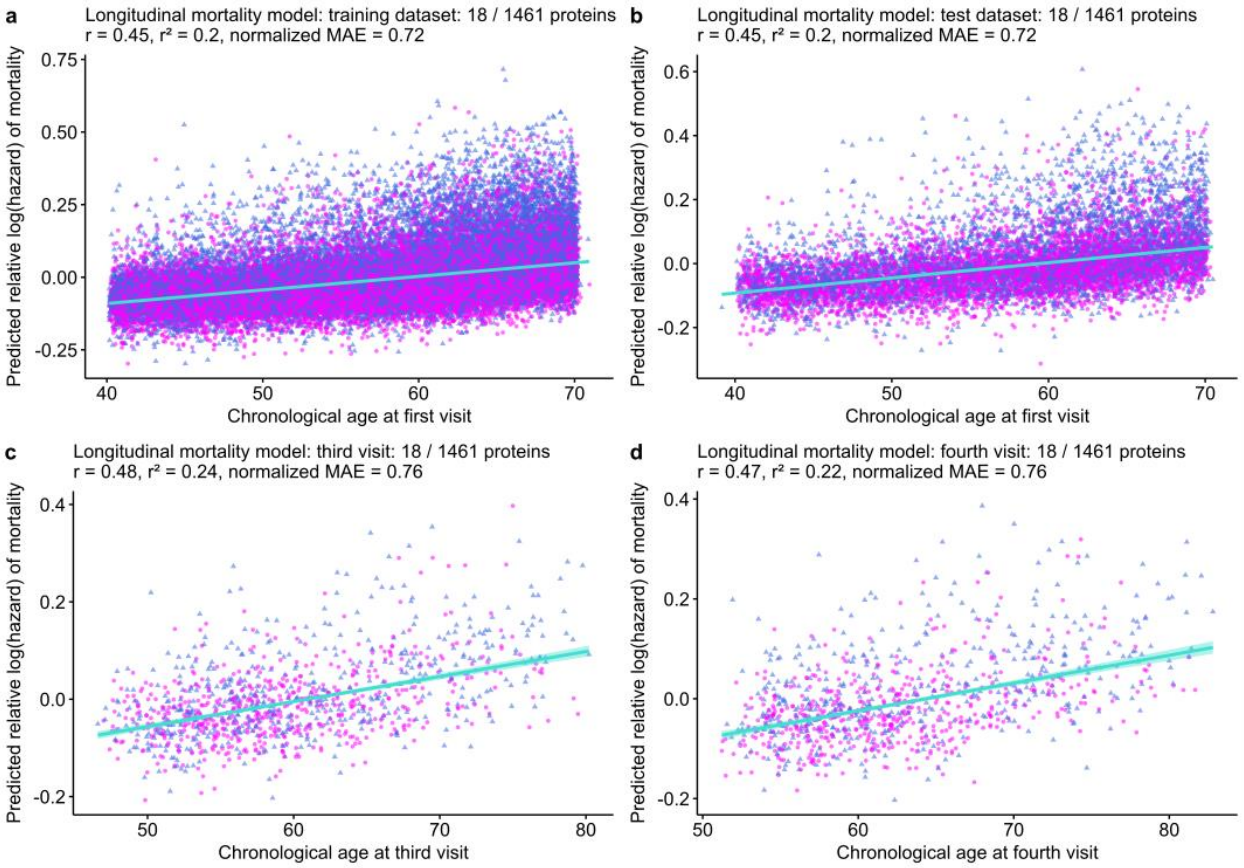

Supplementary Figure 9. Longitudinal mortality-based models associate with chronological age. a. Relative log(hazard) of mortality as predicted by the conventional longitudinal mortality-based aging model correlates positively with chronological age in the training dataset (*n* = 42,412 UK Biobank participants). **b.** Relative log(hazard) of mortality as predicted by the conventional longitudinal mortality-based aging model correlates positively with chronological age in the test dataset (*n* = 10,603 UK Biobank participants). **c.** Relative log(hazard) of mortality as predicted by the conventional longitudinal mortality-based aging model correlates positively with chronological age for the *n* = 1132 UK Biobank participants that have proteomics data available for their third visit. **d.** Relative log(hazard) of mortality as predicted by the conventional longitudinal mortality-based aging model correlates positively with chronological age for the *n* = 1006 UK Biobank participants that have proteomics data available for their fourth visit. r: correlation coefficient, r²: coefficient of determination, normalized MAE: mean absolute error of the normalized residuals, magenta: women, blue: men. Robust regression lines with 95% confidence bands (shaded area) are added.

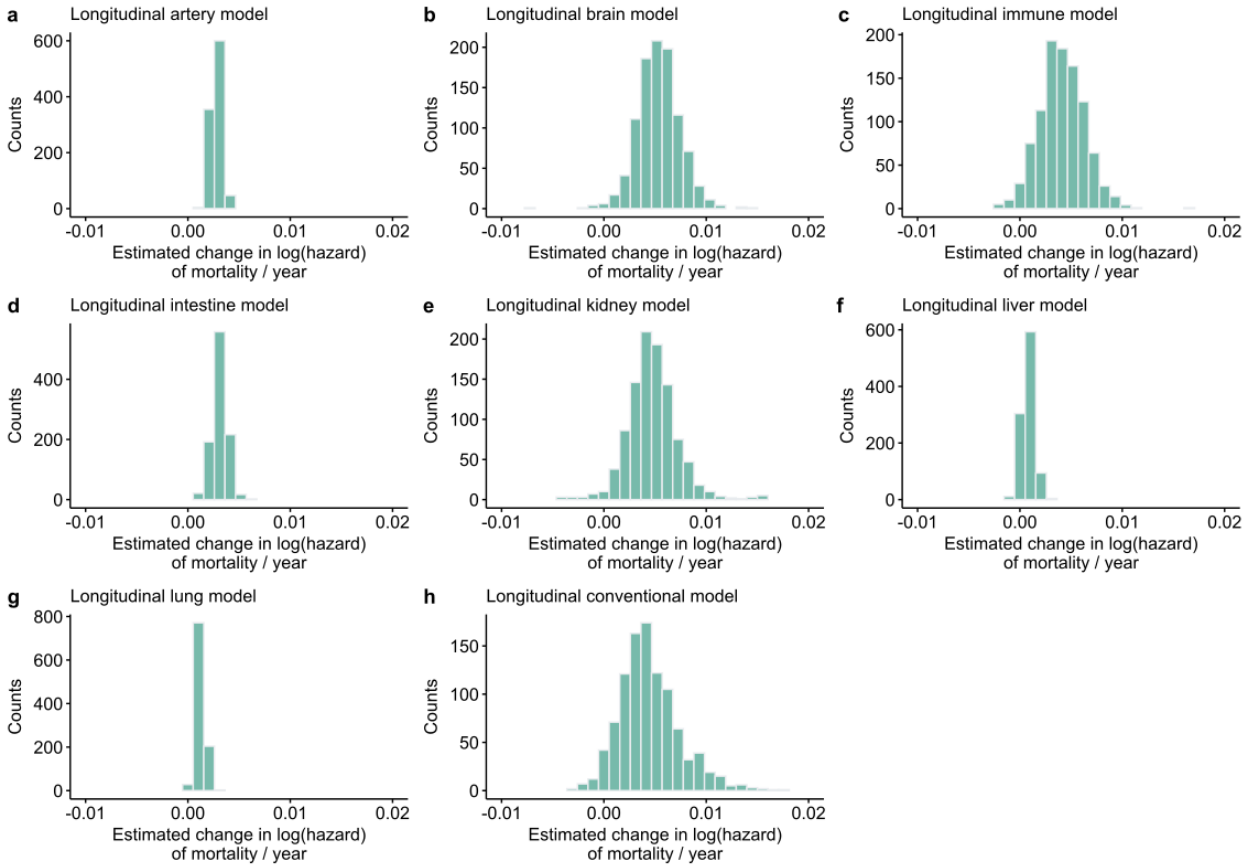

Supplementary Figure 10. The estimated rates of aging as measured by longitudinal mortality-based aging models are mostly positive. The histograms show the distributions of the slopes of the biological ages predicted by the conventional and organ-specific mortality-based models for the *n* = 1,006 individuals that have proteomics data available for their first, third and fourth visits.

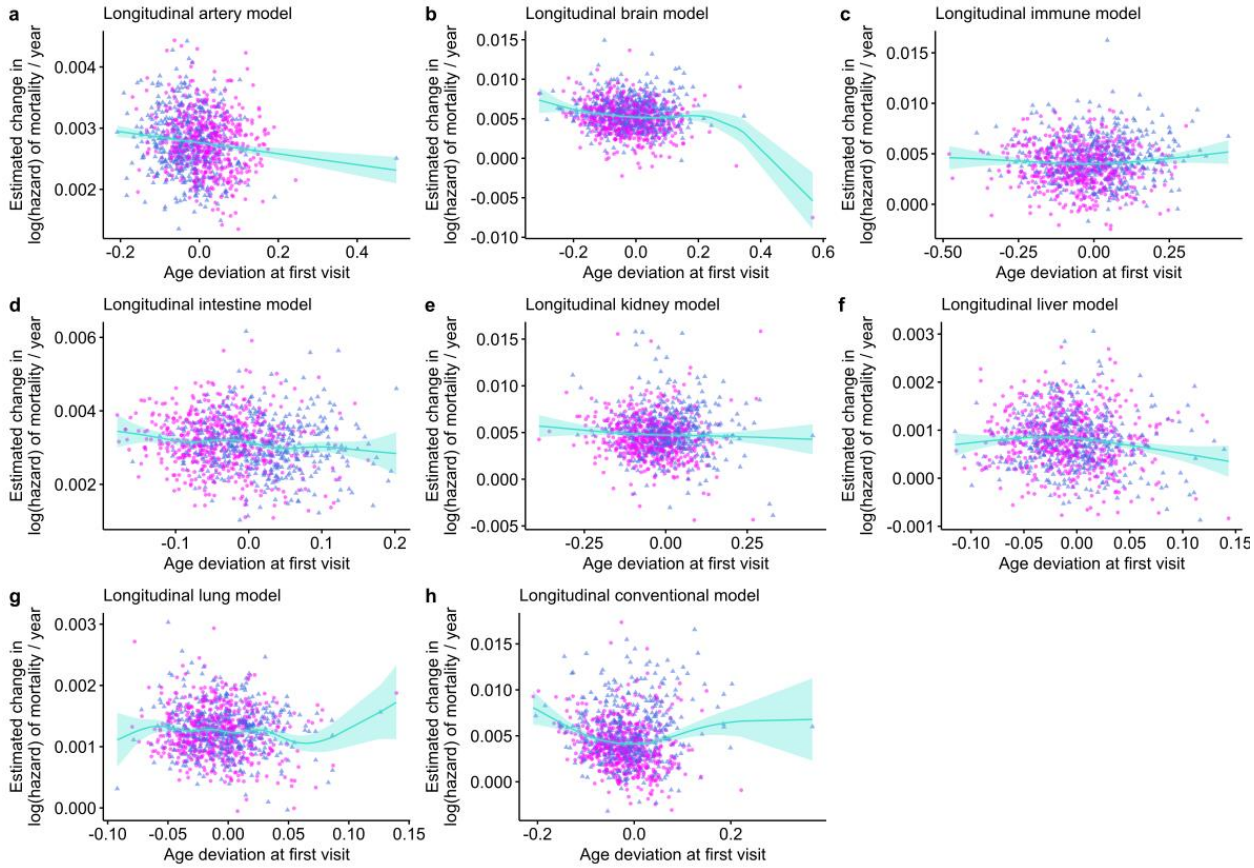

Supplementary Figure 11. For most organ-specific mortality-based models, there is no clear association between the age deviation at first visit and the rate of aging. Effects of age deviation at first visit on the rate of aging as measured by longitudinal mortality-based aging models.

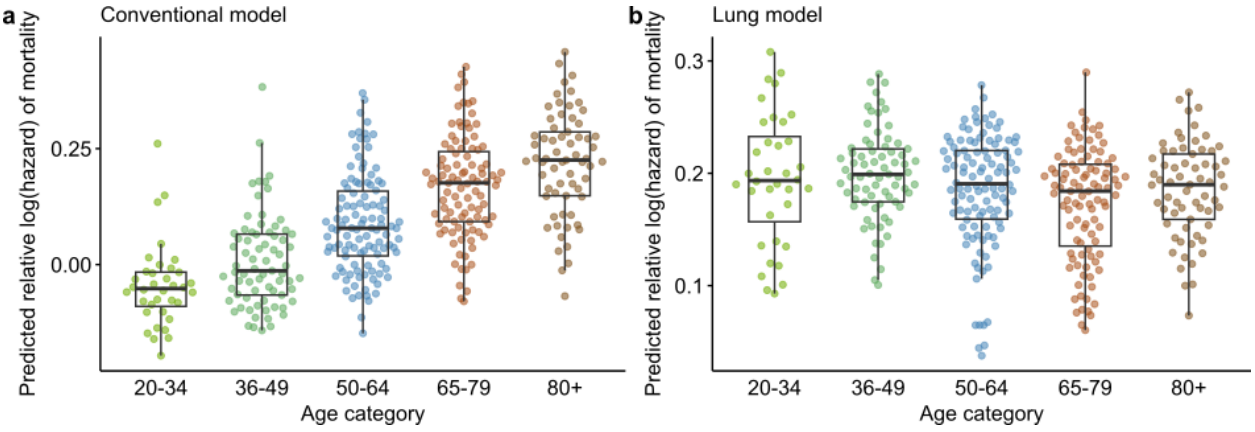

Supplementary Figure 12. The conventional, but not the lung-specific mortality-based model associate with chronological age. a. Data is from the Filbin et al. (2021) dataset. The mortality hazard predicted by the conventional model strongly associates with age (ordinary least squares p value < $1*10^{-16}$, r = 0.62). **b.** The mortality hazard predicted by the lung model shows a slightly negative significant age association (ordinary least squares p value = 0.01, r = 0.13).

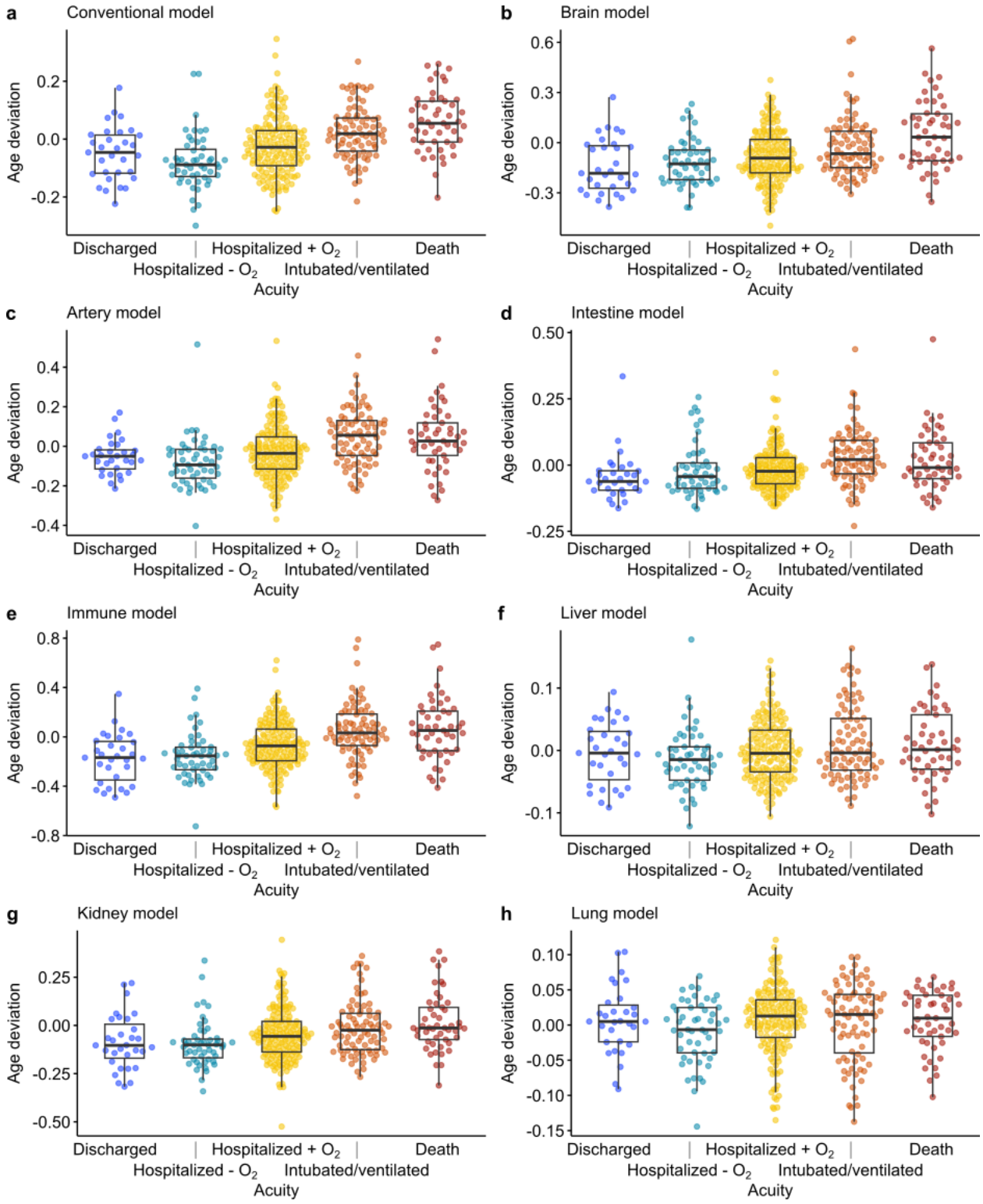

Supplementary Figure 13. Biological age deviations as predicted by the conventional mortality-based model and all organ-specific models except lung associate with increased COVID severity. Ordinary linear regression p-values with Hommel correction: $2*10^{-12}$ (conventional model), $7*10^{-9}$ (brain model), $9*10^{-8}$ (artery model), $1*10^{-4}$ (intestine model), $5*10^{-12}$ (immune model), 0.02 (liver model), $1*10^{-5}$ (kidney model), and 0.5 (lung model). "Discharged": patients not hospitalized and survived to 28 days (*n* =

31), “hospitalized - O_2”: patients hospitalized, but no supplementary oxygen required and survived to 28 days (*n* = 51), “hospitalized + O_2”: patients hospitalized, but supplementary oxygen was required and survived to 28 days (*n* = 169), “Intubated/ventilated”: patients hospitalized and intubated and/or ventilated, and survived to 28 days (*n* = 83). “Death”: patients died within 28 days (*n* = 49).

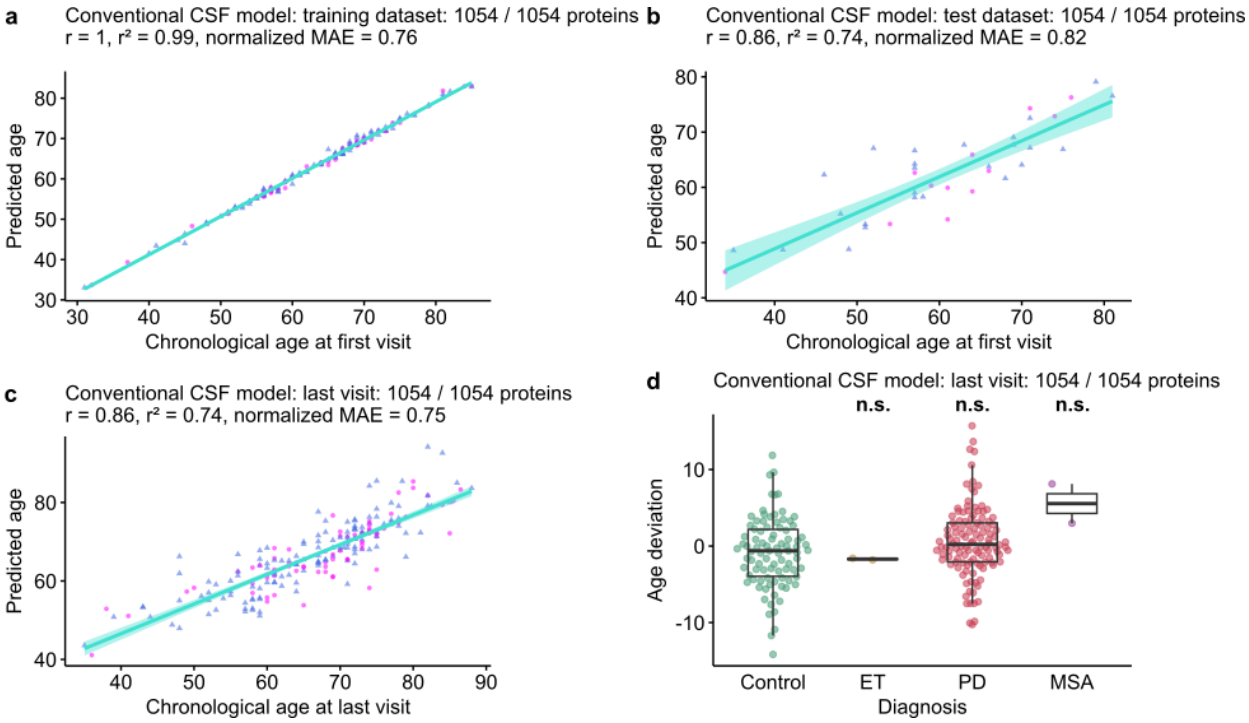

Supplementary Figure 14. Performance of a conventional chronological aging model trained on the CSF proteome. Data is from the Dammer et al. (2022) dataset. **a – b.** Biological ages predicted by the conventional aging model trained on CSF data correlate positively with chronological age in the CSF training and test samples (*n* = 147 and 37 individuals for the training and test datasets, respectively). The number of proteins with non-zero coefficients is shown as a fraction of the total number of proteins on which the models are trained. r: correlation coefficient, r²: coefficient of determination, normalized MAE: mean absolute error of the normalized residuals, magenta: women, blue: men. Robust regression lines with 95% confidence bands (shaded area) are added. **c.** Biological ages predicted by the conventional aging model trained on CSF data correlate positively with chronological age in the CSF samples taken at the last visit (*n* = 212 individuals). r: correlation coefficient, r²: coefficient of determination, normalized MAE: mean absolute error of the normalized residuals, magenta: women, blue: men. Robust regression lines with 95% confidence bands (shaded area) are added. **d.** Biological ages predicted by the conventional aging model trained on CSF data do not differ significantly in age deviation in the essential tremor (ET) group (*n* = 2 individuals), the Parkinson’s disease (PD) group (*n* = 118 individuals), and the multiple systems atrophy (MSA) group (*n* = 2 individuals), as compared to the control group (*n* = 90 individuals) (single-step-adjusted p = 1, 0.07, and 0.1, respectively).

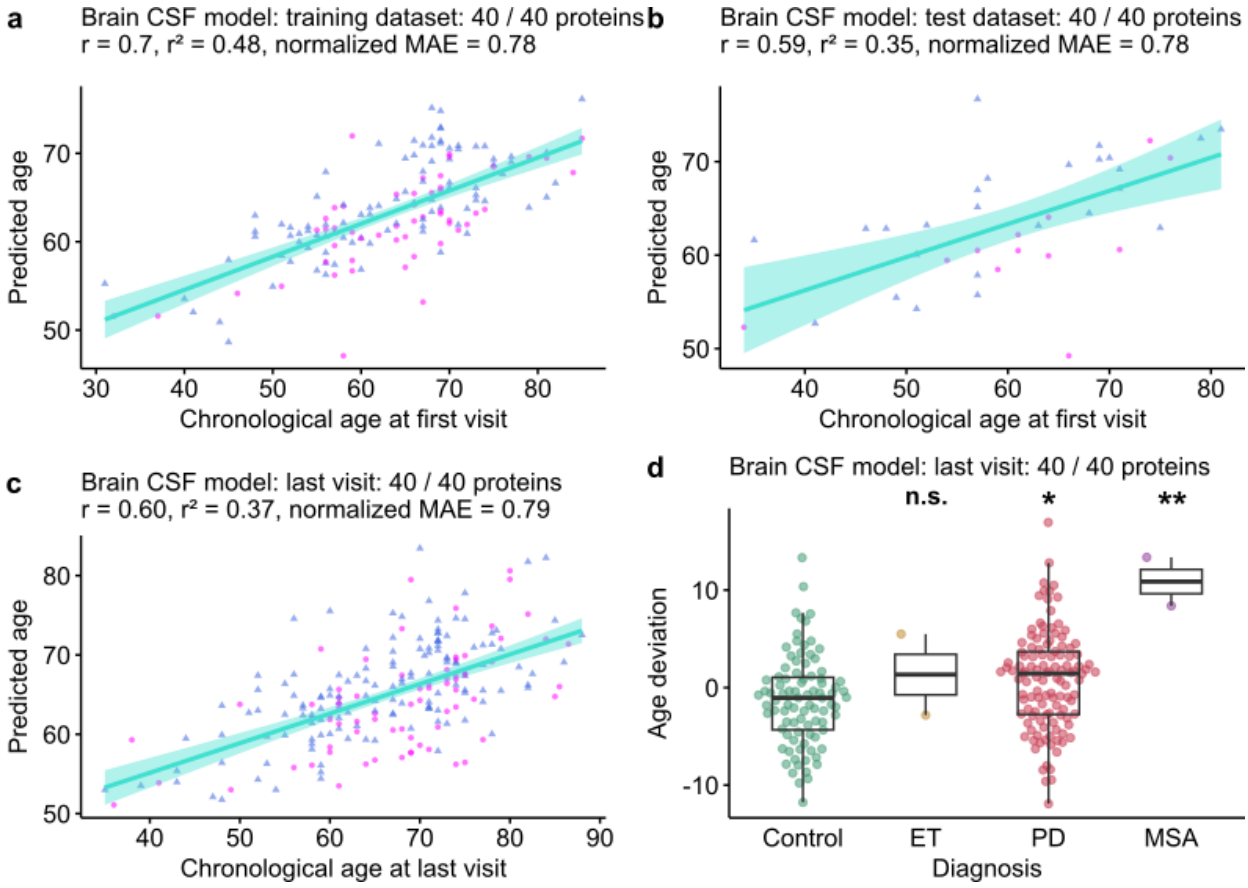

Supplementary Figure 15. Performance of a brain-specific chronological aging model trained on the CSF proteome. Data is from the Dammer et al. (2022) dataset. **a – b.** Biological ages predicted by the brain-specific aging model trained on CSF data correlate positively with chronological age in the CSF training and test samples (*n* = 147 and 37 individuals for the training and test datasets, respectively). The number of proteins with non-zero coefficients is shown as a fraction of the total number of proteins on which the models are trained. r: correlation coefficient, r²: coefficient of determination, normalized MAE: mean absolute error of the normalized residuals, magenta: women, blue: men. Robust regression lines with 95% confidence bands (shaded area) are added. **c.** Biological ages predicted by the brain-specific aging model trained on CSF data correlate positively with chronological age in the CSF samples taken at the last visit (*n* = 212 individuals). r: correlation coefficient, r²: coefficient of determination, normalized MAE: mean absolute error of the normalized residuals, magenta: women, blue: men. Robust regression lines with 95% confidence bands (shaded area) are added. **d.** Biological ages predicted by the brain-specific aging model trained on CSF data do not differ significantly in age deviation in the essential tremor (ET) group (*n* = 2 individuals), the Parkinson's disease (PD) group (*n* = 118 individuals), and the multiple systems atrophy (MSA) group (*n* = 2 individuals), as compared to the control group (*n* = 90 individuals) (single-step-adjusted p = 0.8, 0.01, and 0.002, respectively).

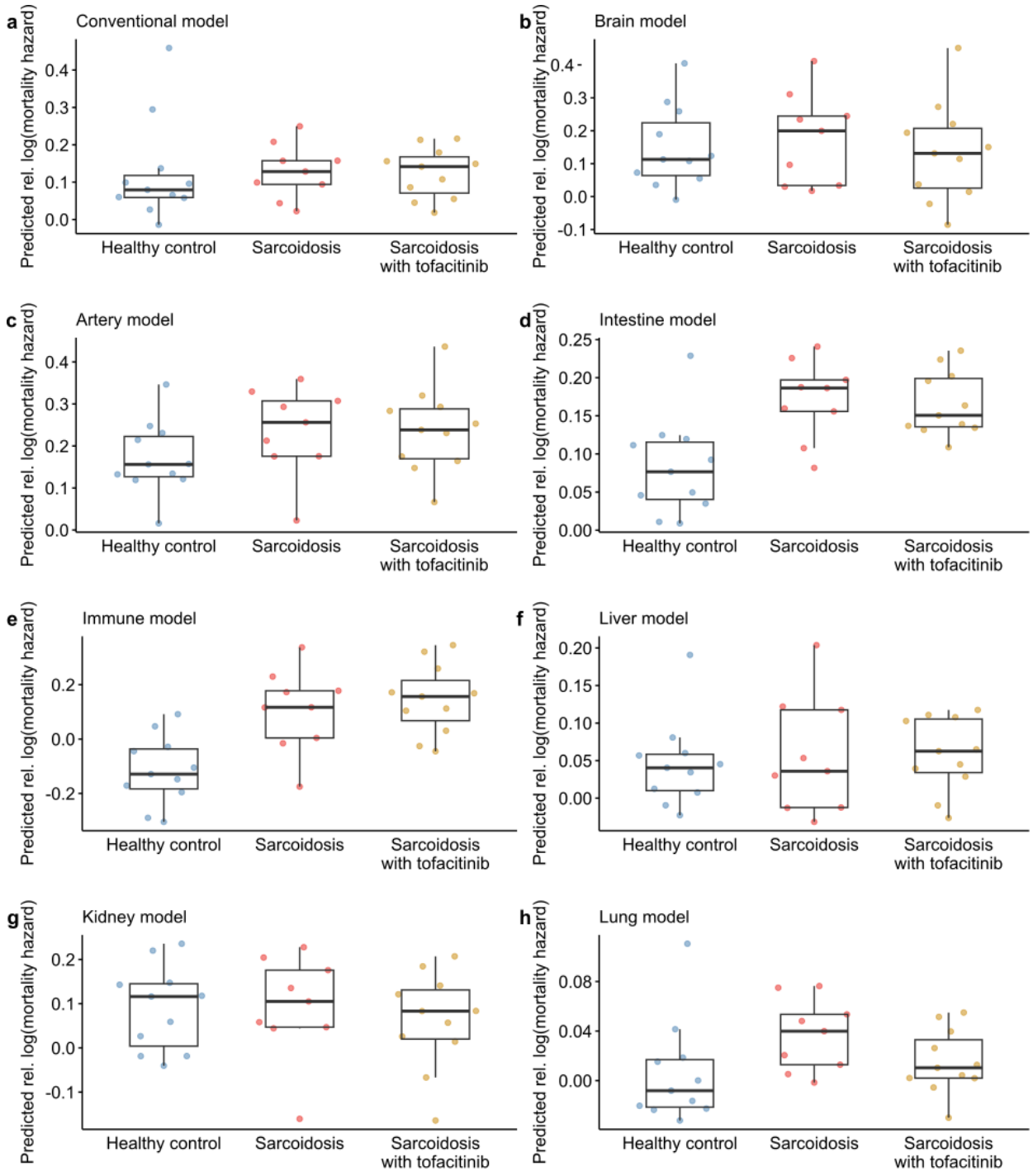

Supplementary Figure 16. The mortality-based immune and intestine aging models associate with sarcoidosis. Relative log(hazards) of mortality as predicted by the mortality-based conventional and organ-specific aging models based on the plasma proteomics of 11 healthy controls, 9 untreated sarcoidosis patients, and 11 sarcoidosis patients treated with tofactinib, measured with the Olink Explore 1536 platform in the dataset of Damsky et al. (2022). Ordinary linear regression p-values with Hommel correction for the comparison sarcoidosis with or without tofacitinib vs healthy controls: 0.9 (conventional model), 0.9 (brain model), 0.4 (artery model), 0.001 (intestine model), 0.001 (immune model), 0.9 (liver model), 0.9 (kidney model), and 0.6 (lung model).